

# Structural characterization of nitrided 34CrAlNi7 steel

A. Türk\*, O. Ok

*Sakarya University, Engineering Faculty, Department of Metallurgical and Materials Engineering, Esentepe Campus  
54187, Adapazari, Turkey*

Received 20 October 2006, received in revised form 4 February 2009, accepted 4 February 2009

## Abstract

The nitriding behaviour of 34CrAlNi7 alloy steel was investigated under three different nitriding processes. One of them is salt-bath nitriding that was carried out at a temperature of 525 °C for treatment time of 1, 2 and 3 h. The others are ion nitriding and fluidized bed nitriding that were conducted at 500 °C and 540 °C, respectively, in treatment time of 6, 12 and 18 h. The thickness of compound layer, measured by means of a digital thickness instrument attached to optical microscope, ranged from 3 µm to 16 µm depending on nitriding technique and treatment time. The presence of  $\gamma'$ -Fe<sub>4</sub>N and  $\varepsilon$ -Fe<sub>2-3</sub>N phases formed in the compound layer was confirmed by XRD analysis. Kinetics studies showed that the effective diffusion coefficients are  $453 \times 10^{-14}$ ,  $77.8 \times 10^{-14}$  and  $278 \times 10^{-14}$  m<sup>2</sup> s<sup>-1</sup> for salt bath, plasma and fluidized bed processes, respectively.

**Key words:** plasma nitriding, fluidized bed nitriding, 34CrAlNi7 steel

## 1. Introduction

Nitriding is a ferritic thermochemical treatment that is very widely used for engineering components in order to improve their wear properties, corrosion resistance and fatigue life [1]. This process is carried out relatively at low temperature, usually in the range 480–600 °C, and it does not change phase structure of the steel. Thus, there is minimal distortion because no phase changes occur in the steel. The nitriding process has been successfully applied to carbon steels, alloy steels, tool steels, and stainless steels [1–10]. Gas nitriding and salt-bath nitriding have been used by engineers to improve the surface properties of parts and components in a number of different industries for many years [11]. In addition, new techniques of the nitriding have been developed in recent years, known as ion (or plasma) nitriding and fluidized bed nitriding.

Conventional nitriding causes the formation of a relatively thick diffusion layer with a fine dispersion of alloy nitrides as well as a thin compound or white layer on the component surface [1]. The compound layer consists of a heterogeneous mixture of  $\gamma'$ -Fe<sub>4</sub>N and  $\varepsilon$ -Fe<sub>2-3</sub>N phases. Even though this layer has a relatively high hardness of 900–1000 HV and good

frictional characteristics, high internal stresses make it friable and brittle, which can often lead to spalling during service [1, 12].

Ion nitriding has many advantages compared to the traditional nitriding processes, such as short treatment time, low process temperature, minimal distortion, clean specimens and low energy use [1, 5, 12]. This process also decreases thickness of compound layer and reduces the tendency of spalling [1].

Fluidized bed technology has been successfully used for nitriding and other thermochemical coatings. This method is simple, efficient and environmentally friendly and it has high rates for mass and heat transfer [13].

In this study, structural characterization of the nitrided 34CrAlNi7 steel with three different nitriding techniques, salt-bath nitriding, ion nitriding and nitriding in fluidized bed, was investigated.

## 2. Experimental details

The material used in this investigation was commercial 37CrAlNi7 steel, quenched from 860 °C in oil and tempered at 575 °C before nitriding process. The

\*Corresponding author: tel.: +90 264 295 57 73; fax: +90 264 295 56 61; e-mail address: [aturk@sakarya.edu.tr](mailto:aturk@sakarya.edu.tr)

composition of the steel was (wt.%): C, 0.35; Cr, 1.7; Mo, 0.20; Al, 1.0; Ni, 1.0; and Fe, balance. Specimens were sawed in running water in the form of rectangular substrates of size  $(15 \times 10 \times 5) \text{ mm}^3$ . The surfaces of the substrates were mechanically ground using 100, 320, 400, and 600 grit SiC papers and cleaned alcohol before nitriding.

Plasma nitriding treatment was performed commercially in a D.C. glow discharge plasma nitriding system, at  $500^\circ\text{C}$  for 6, 12 and 18 h of nitriding time in a 100 %  $\text{NH}_3$  gas atmosphere at total pressure of 10 mbar. Liquid nitriding was also carried out commercially by Sulfinuz method in a NaCN salt bath at a temperature of  $525^\circ\text{C}$  for treatment time of 1, 2 and 3 h.

The nitriding in fluidized bed furnace containing  $\text{Al}_2\text{O}_3$  as a gas carrier was made at a temperature of  $540^\circ\text{C}$  for treatment time of 6, 12 and 18 h in a mixture of 40% $\text{NH}_3$ -60% $\text{N}_2$  industrially. The fluidized bed phenomenon is the one in which a bed of particles, e.g.  $\text{Al}_2\text{O}_3$ , behaves like a liquid, when a moving gas is fed through the bed [14]. Some of the parameters that affect the quality of fluidization in a fluidized bed reactor are the properties of fluids used, the bed geometry, gas flow rate.

After the nitriding processes, microstructural examination was conventionally made on ground and polished samples using optical microscope. The samples were etched in 3 % nital solution and Oberhofer etching agent. More detailed investigation of metallographic structures was carried out using a JEOL JSM 6060-LV type scanning electron microscope (SEM). The compound layer thickness that formed on the steel surface was measured by using a digital instrument attached to optical microscope. Surface phase analyses of the samples were carried out by a Shimadzu XRD-6000 Model X-ray diffractometer using a Cu  $K\alpha$  radiation with wavelength of  $1.5406 \text{ \AA}$ .

The case depth and hardness of surface and sub-surface were determined using a Leitz microhardness tester at an applied load of 50 g and a time of 20 s. The case depth was defined as the depth that the hardness was 50 HV above the core hardness.

### 3. Results

#### 3.1. Microstructure

Figure 1 shows optical micrograph of the cross section of steel nitrided by different process. The outermost layer, very thin and consisting of chiefly iron nitrides, is generally referred to as a white layer or compound layer. It was found that the compound layer thickness increased with increasing nitriding time. Depending on nitriding time the layer thickness was obtained in the range of 3–6  $\mu\text{m}$  for plasma nitriding and

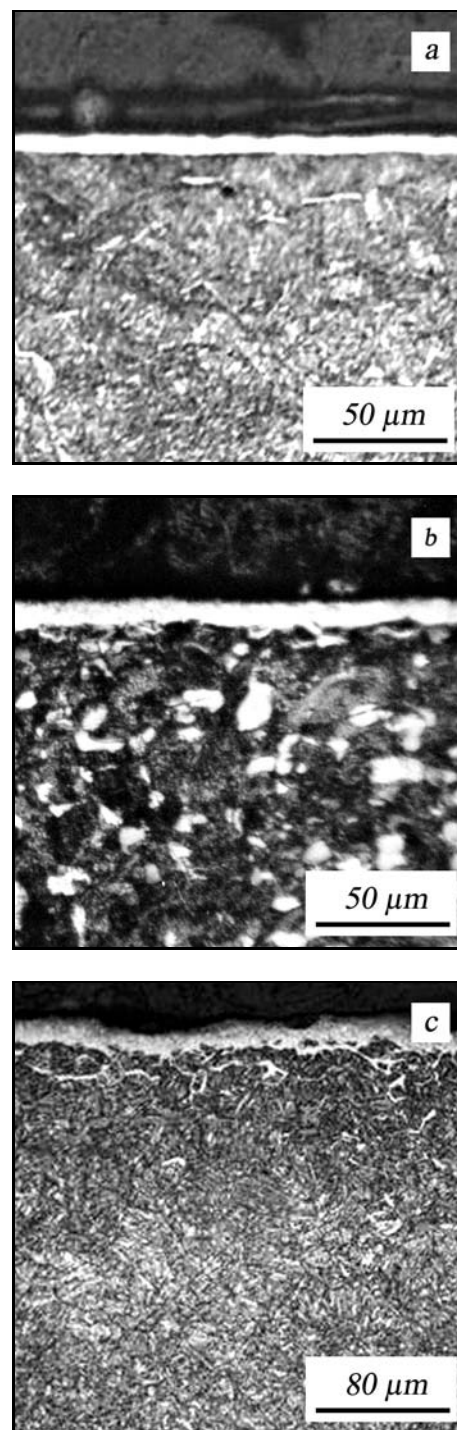


Fig. 1. Optical micrographs of 34CrAlNi7 steel nitrided in plasma at  $500^\circ\text{C}$  for 12 h (a), salt bath at  $525^\circ\text{C}$  for 2 h (b) and fluidized bed at  $540^\circ\text{C}$  for 12 h (c).

4.5–8  $\mu\text{m}$  for salt bath nitriding, respectively. It was found that the layer thickness ranged 11.5–16  $\mu\text{m}$  in fluidized bed nitriding is higher than others.

The layer located under the compound layer is called diffusion zone. In this zone, nitrogen has mainly been incorporated into the existing iron lattice as in-

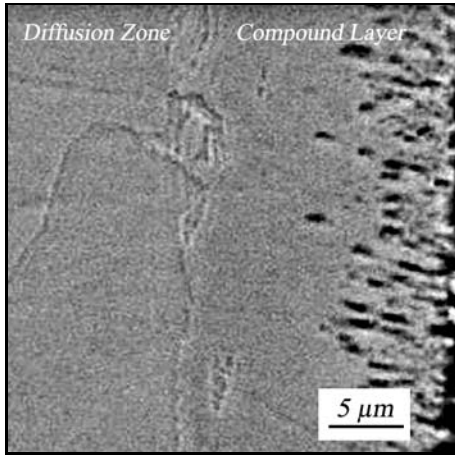


Fig. 2. SEM image of 34CrAlNi7 steel nitrided in salt bath at 525 °C for 3 h.

terstitial atoms or as finely dispersed alloy nitride precipitates [5]. The thickness of the diffusion zone depends on the process temperature, time and chemical composition of the steel.

The cross-sectional SEM image of the 34CrAlNi7 steel nitrided in salt bath at 525 °C for 3 h is presented in Fig. 2. In this figure, the effect of nitriding on the steel surface was clearly observed. The steel sample has a compound layer on the surface, which appears to grow from acicular precipitates that merge to form a dense nitride layer as the treatment is in progress. The diffusion zone can be observed underneath this layer.

### 3.2. Layer thickness and hardness

The values of compound layer thickness, case depth, growth rate of case layer and surface hardness of the steel depending on nitriding process are presented in Table 1. The variation of square of diffusion

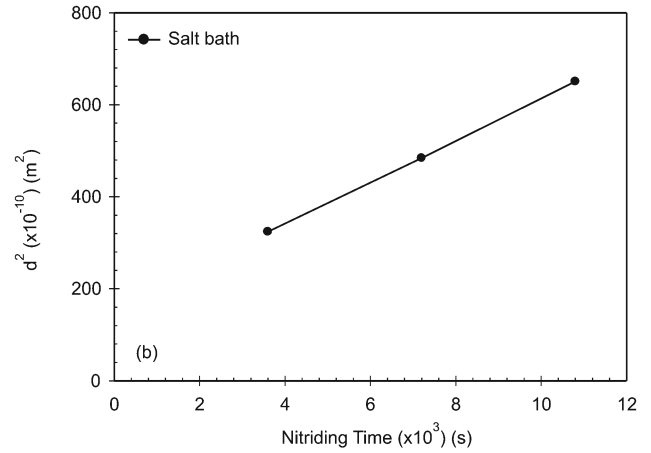
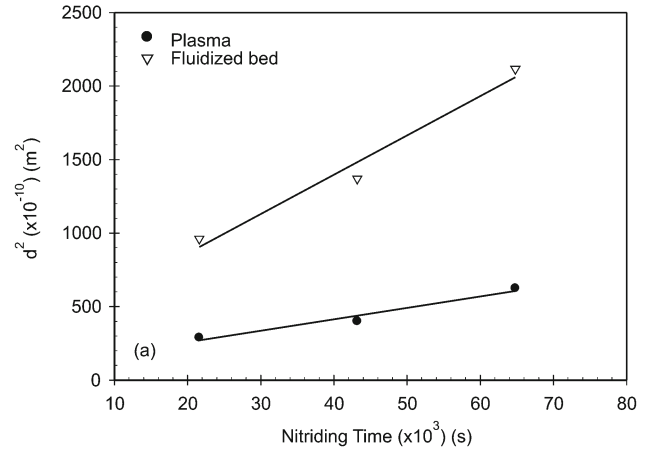


Fig. 3. The variation of diffusion zone as a function of process time: (a) plasma and fluidized bed, (b) salt bath nitriding.

zone as a function of process time is shown in Fig. 3. As it can be seen in Fig. 3 and Table 1, the case depth increases with increasing nitriding time for each three processes. The maximum case depth was observed in

Table 1. The change of the compound layer thickness, the case depth, growth rates of case layer and surface hardness with the nitriding process in the 34CrAlNi7 steel

Nitriding process	Temperature (°C)	Time (h)	Compound layer thickness (μm)	Case depth (μm)	Growth rates of case layer (μm h <sup>-1</sup> )	Surface hardness (HV)
Plasma	500	6	3.0	170	28.33	965
		12	5.0	200	16.66	1225
		18	6.0	250	13.88	1253
Salt bath	525	1	4.5	180	180	1100
		2	6.0	220	110	1150
		3	8.0	255	85	1225
Fluidized bed	540	6	11.5	310	51.66	1080
		12	13.8	360	30.00	1150
		18	16.0	465	25.83	1215

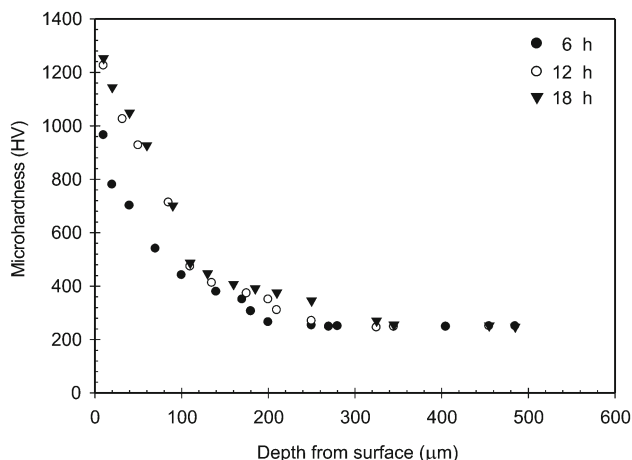


Fig. 4. Microhardness profiles of nitrided 34CrAlNi7 in plasma for different nitriding time.

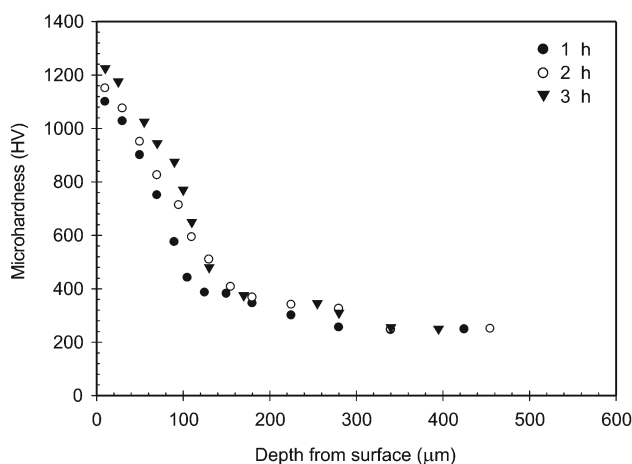


Fig. 5. Microhardness profiles of nitrided 34CrAlNi7 in salt bath for different nitriding time.

the fluidized bed nitriding at a temperature of 540 °C and a time of 18 h.

From the slope of square case depth versus the nitriding time plots given in Fig. 3, effective diffusion coefficient was calculated according to  $d^2 = Dt$  equation, where  $t$  is nitriding time,  $d$  is the case depth and  $D$  is the diffusion coefficient. The effective diffusion coefficients are found to be approximately  $453 \times 10^{-14}$ ,  $77.8 \times 10^{-14}$  and  $278 \times 10^{-14} \text{ m}^2 \text{ s}^{-1}$  for salt bath, plasma and fluidized bed processes, respectively. The growth rate of the case layer was also calculated from case depth divided by nitriding time (Table 1). The growth rate of the case layer decreased with increasing nitriding time in each process.

The hardness profiles of nitrided samples as a function of case depth for nitriding processes are given in Figs. 4–6. The hardness continuously decreases from

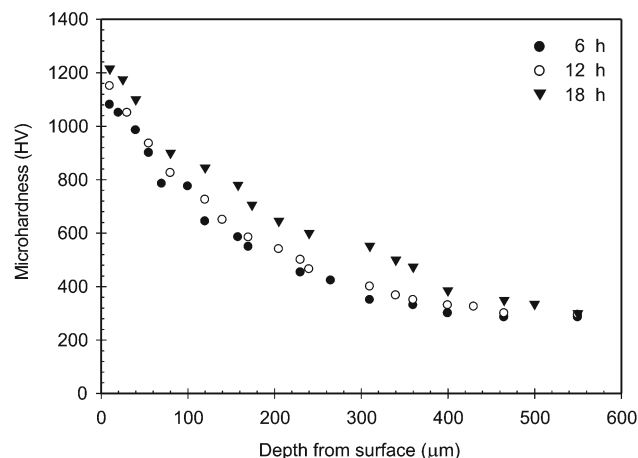


Fig. 6. Microhardness profiles of nitrided 34CrAlNi7 in fluidized bed for different nitriding time.

Table 2.  $2\theta$  positions for all of the phases confirmed by XRD

Nitriding process	Phases	$2\theta$ position
Plasma	$\epsilon$	38.25; 41.03; 43.53; 57.26; 69.34; 76.42
	$\gamma'$	41.03; 47.82; 68.28
	$\alpha$ -Fe	44.24
Salt bath	$\epsilon$	37.72; 40.8; 43.1; 56.85; 69.77; 76.16
	$\gamma'$	40.8; 47.64; 68.32
Fluidized bed	$\epsilon$	36.85; 40.72; 56.55; 64.74; 69.61
	$\gamma'$	40.72; 47.45; 69.61
	$\alpha$ -Fe	44.1; 62.15
	$\text{Cr}_2\text{N}$	29.71

surface to core due to decreasing of nitrogen concentration. In the plasma nitriding, the maximum surface hardness was obtained as 1253 HV at a temperature of 500 °C for 18 h. The maximum surface hardness is 1215 HV and 1225 HV for salt bath and fluidized bed, respectively.

### 3.3. Characterization

X-ray diffraction patterns of nitrided steel in plasma and fluidized bed at 500 °C and 540 °C for 12 h, respectively, and salt bath at 525 °C for 2 h are shown in Fig. 7. As can be seen from Fig. 7b,  $\text{Fe}_{2-3}\text{N}$  ( $\epsilon$ ) and  $\text{Fe}_4\text{N}$  ( $\gamma'$ ) phases formed on surface of the steel nitrided in salt bath. In addition to  $\gamma'$  and  $\epsilon$  phases, peaks of  $\alpha$ -Fe phase were obtained from XRD patterns of nitrided steel in plasma process (Fig. 7a). In addition to these phases,  $\text{Cr}_2\text{N}$  phase formed on the

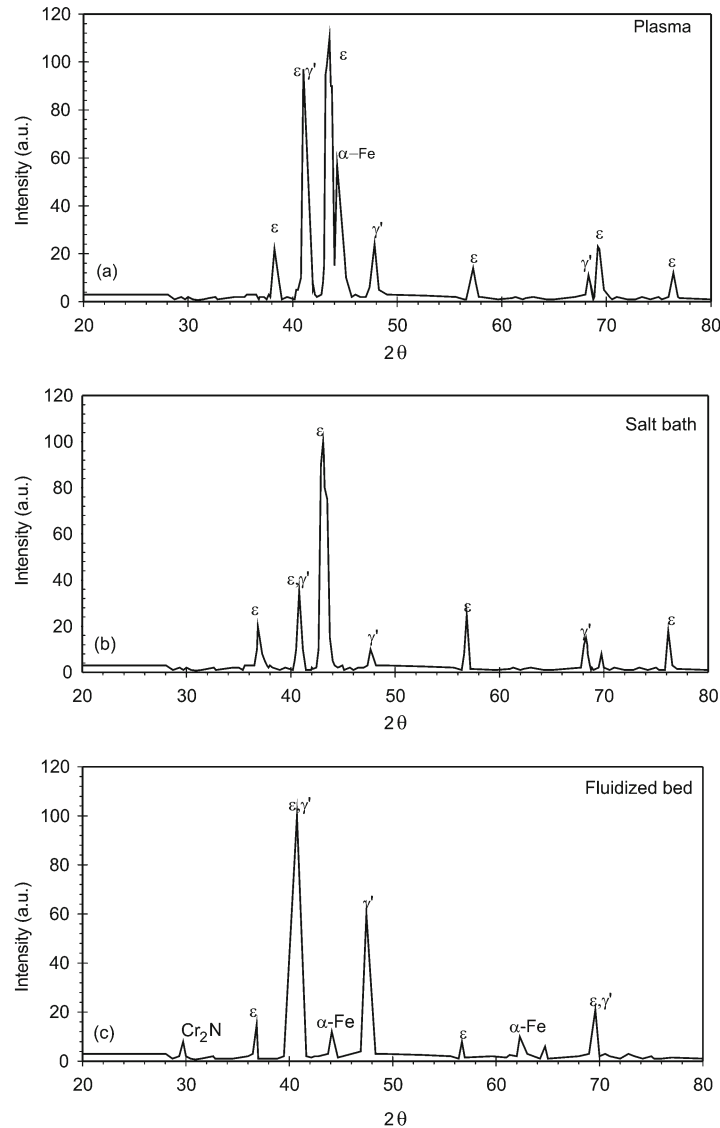


Fig. 7. XRD patterns of the steel nitrided in plasma at 500°C for 12 h (a), salt bath at 525°C for 2 h (b) and fluidized bed at 540°C for 12 h (c).

surface of the steel nitrided in fluidized bed process (Fig. 7c). Depending on nitriding processes,  $2\theta$  positions for all phases confirmed by X-ray diffraction analysis technique were listed in Table 2. It can be said that the ratio of  $\epsilon$  and  $\gamma'$  phases formed on surface of steel nitrided in salt bath is higher than that of other processes from the comparison between Fig. 7b and Figs. 7a,c.

#### 4. Discussion

The above results showed that the coatings performed by fluidized bed, plasma and salt bath nitriding had uniform morphology. The diffusion zone of a nitrided case can be described as the original core

microstructure with some solid solution and precipitation strengthening. It is known that the nitrogen exists in the form of single atoms in interstitial positions until the limit of nitrogen solubility exceeds  $\cong 0.4$  wt.% N in pure iron. This solid solution strengthening zone is only slightly harder than the core. The depth of diffusion zone depends on the N concentration gradient, time and the chemical composition of the steel at a given temperature [15]. As the N concentration increases toward the surface, very fine, coherent nitride precipitates are formed when the solubility limit of N is reached [16]. The precipitates can exist both in the grain boundaries and within the grains. These precipitates, nitrides of iron or alloying elements distort the lattice and pin crystal dislocations and thereby substantially increase the hardness of the materials. Es-

pecially, Ti, Al, V, Cr, Mo, and W can combine with N to form metallic nitrides in terms of thermodynamic hierarchy [17].

It was observed that the hardness of nitride layer was much higher than that of the matrix (Figs. 4–6). This is a consequence of the presence of hard  $\text{Fe}_4\text{N}$ ,  $\text{Fe}_{2-3}\text{N}$  and  $\text{Cr}_2\text{N}$  nitrides as determined by XRD analysis (Fig. 7). For example, the hardness of nitride layer was found to be between 965–1253 HVN depending on nitriding process and time whereas the hardness of substrate was 300 HVN.

In this study, the process temperature and the test materials are fixed, but process and time parameters were variable. Depending on nitriding time, diffusion zone depths were obtained as 170–250  $\mu\text{m}$ , 180–255  $\mu\text{m}$  and 310–465  $\mu\text{m}$  for plasma, salt bath and fluidized bed processes, respectively. Kinetic studies showed that the effective diffusion coefficients for 34CrAlNi7 steel depended considerably on nitriding processes. These are  $77.8 \times 10^{-14}$ ,  $453 \times 10^{-14}$  and  $278 \times 10^{-14} \text{ m}^2 \text{ s}^{-1}$  for plasma, salt bath and fluidized bed processes, respectively. It is possible to say that these experimentally measured diffusion coefficient values reveal the bulk diffusion process for the steel [18, 19]. Also, it is possible to claim that there is a close relationship between layer thickness and nitriding process. Especially, the thickness of layer is very important for fatigue applications, because the increasing case depth increases the fatigue limit of the steels [20–22]. The white layer has no effect on the fatigue limit, but it increases the wear resistance of nitrided steels owing to its layered crystal structure.

The growth rate of case layer was calculated dividing the case depth by nitriding time (Table 1). It decreased with increasing nitriding time in each process. It can be seen from Table 1, that the growth rate in the salt bath is higher than that of the other processes because the salt bath process has high mass and heat transfer rates, and the lowest growth rate was obtained in plasma process. The reactivity of salt baths combined with their heat capacity and direct contact with the steel surface create better possibilities for nitrogen penetration than in gas nitriding [23]. Plasma nitriding is a process of surface hardening using glow discharge technology to introduce nascent nitrogen to the surface of a metal part for subsequent diffusion into the materials. As it is well known, the lower nitrogen content, the lower compound layer for plasma nitriding depends on process atmosphere. However nitriding time in plasma has to be higher than in salt bath for higher layer thickness.

In this study, the deepest diffusion layer was obtained in the fluidized bed nitriding and surface hardness of the steel nitrided in fluidized bed is similar to that of the nitrided in other processes (Table 1), and the hardness distribution of steel nitrided in this process is more regular than that of the others (Figs. 4–6).

Moreover, in fluidized bed, the growth rate of the diffusion layer is higher than that of the plasma.

## 5. Conclusions

1. The maximum surface hardness was obtained for the nitriding time of 18 h in plasma and fluidized bed, while the maximum surface hardness was obtained for 3 h in salt bath.
2. The deepest diffusion zone thickness was obtained in fluidized bed after 18 h nitriding process.
3. The compound layer thickness increased with increasing nitriding time, and layer thickness was obtained in the range of 3–16  $\mu\text{m}$  depending on nitriding process.
4. XRD analysis confirmed the presence of  $\text{Fe}_4\text{N}$ ,  $\text{Fe}_{2-3}\text{N}$ ,  $\text{Cr}_2\text{N}$ , and  $\alpha\text{-Fe}$  in coating layer.
5. It was found that the effective diffusion coefficients for 34CrAlNi7 steel depended considerably on the nitriding processes.

## Acknowledgements

The authors would like to thank Prof. Dr. Cuma Bindal for his scientific comments and support in this research.

## References

- [1] PODGORNIK, B.—VIZINTIN, J.—LESKOVSEK, V.: Surf. Coat. Technol., 108–109, 1998, p. 454.
- [2] FERKEL, H.—GLATZER, M.—ESTRIN, Y.—VALIEV, R. Z.: Scrip. Mater., 46, 2002, p. 623.
- [3] BLAWERT, C.—MORDIKE, B. L.—HUCHEL, U.—STRAMKE, S.—COLLINS, G. A.—SHORT, K. T.—TENDYS, J.: Surf. Coat. Technol., 98, 1998, p. 1181.
- [4] DEVI, M. U.—CHAKRABORTY, T. K.—MOHANTY, O. N.: Surf. Coat. Technol., 116–119, 1999, p. 212.
- [5] ÇELİK, A.—EFEOĞLU, I.—SAKAR, G.: Mater. Charact., 46, 2001, p. 39.
- [6] ALSARAN, A.—ÇELİK, A.: Mater. Charact., 47, 2001, p. 207.
- [7] ALPHONSA, I.—CHAINANI, A.—RAOLE, P. M.—GANGULI, B.—JOHN, P. I.: Surf. Coat. Technol., 150, 2002, p. 263.
- [8] YU, Z.—XU, X.—WANG, L.—QIANG, J.—HEI, Z.: Surf. Coat. Technol., 153, 2002, p. 125.
- [9] MISHRA, S. C.—NAYAK, B. B.—MOHANTY, B. C.: Surf. Coat. Technol., 145, 2001, p. 24.
- [10] ATIK, E.—YUNKER, U.—MERİÇ, C.: Tribology Int., 36, 2003, p. 155.
- [11] PYE, D.: Industrial Heating, March 2001, p. 39.
- [12] PODGORNIK, B.—VIZINTIN, J.: Mater. Sci. Eng., A315, 2001, p. 28.
- [13] ANTHYMIDIS, K. G.—STERGIOUDIS, E.—TSIPAS, D. N.: Mater. Letters, 52, 2001, p. 156.
- [14] SAGON-KING, R. F.: Metals Handbook. ASM International, The Materials Information Society, Materials Park, OH, Vol. 4, 1997, p. 484.

- [15] O'BRIEN, J. M.: *Metals Handbook*. ASM International, The Materials Information Society, Materials Park, OH, Vol. 4, 1997, p. 419.
- [16] BERG, M.—BUDTZ-JORGENSEN, C. V.—REITZ, H.—SCHWEITZ, K. O.—CHEVALLIER, J.—KRINGHOJ, P.—BOTTIGER, J.: *Surf Coat Technol.*, 124, 2000, p. 25.
- [17] WICKS, C. E.—BLOCK, F. E.: *Thermodynamic Properties of 65 Elements – Their Oxides, Halides, Carbides and Nitrides*. Washington, USA Government Printing Office 1963.
- [18] VERHOEVEN, J. D.: *Fundamentals of Physical Metallurgy*. New York, John Wiley and Sons, Inc. 1975.
- [19] TÜRK, A.—OK, O.—BINDAL, C.: *Vacuum*, 80, 2005, p. 332.
- [20] SUN, Y.—BELL, T.: *Mater Sci Eng.*, A140, 1991, p. 419.
- [21] GENEL, K.—DEMIRKOL, M.—ÇAPA, M. : *Mater Sci Eng.*, A279, 2000, p. 207.
- [22] ALSARAN, A.—KARAKAN, M.—ÇELİK, A.: *Mater. Charact.*, 48, 2002, p. 323.
- [23] FUNATANI, K.: *Metal Sci. and Heat Treat.*, 46, 2004, p. 277.